

RD-R176 136

COMPUTER SIMULATION OF DETERIORATION BY
ELECTROMIGRATION (U) RENSSELAER POLYTECHNIC INST TROY NY
H B HUNTINGTON ET AL. SEP 86 RNDC-TR-86-133

1/1

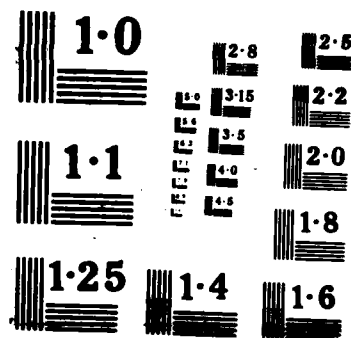
UNCLASSIFIED

F30602-83-C-0194

F/G 11/6

ML





AD-A176 136

RADC-TR-86-133
Final Technical Report
September 1986



COMPUTER SIMULATION OF DETERIORATION BY ELECTROMIGRATION

Rensselaer Polytechnic Institute

H. B. Huntington and S. Ahmad

S JAN 27 1987

A

APPROVED FOR PUBLIC RELEASE; DISTRIBUTION UNLIMITED

DTIC FILE COPY

**ROME AIR DEVELOPMENT CENTER
Air Force Systems Command
Griffiss Air Force Base, NY 13441-5700**

87 1 23 070

This report has been reviewed by the RADC Public Affairs Office (PA) and is releasable to the National Technical Information Service (NTIS). At NTIS it will be releasable to the general public, including foreign nations.

RADC-TR-86-133 has been reviewed and is approved for publication.

APPROVED: *Mark W. Levi*

MARK W. LEVI
Project Engineer

APPROVED: *W. S. Tuthill*

W. S. TUTHILL, Colonel, USAF
Chief, Reliability & Compatibility Division

FOR THE COMMANDER: *John A. Ritz*

JOHN A. RITZ
Plans & Programs Division

If your address has changed or if you wish to be removed from the RADC mailing list, or if the addressee is no longer employed by your organization, please notify RADC (RBRP) Griffiss AFB NY 13441-5700. This will assist us in maintaining a current mailing list.

Do not return copies of this report unless contractual obligations or notices on a specific document requires that it be returned.

UNCLASSIFIED
SECURITY CLASSIFICATION OF THIS PAGE

REPORT DOCUMENTATION PAGE														
1a REPORT SECURITY CLASSIFICATION UNCLASSIFIED		1b RESTRICTIVE MARKINGS N/A RD-1473-136												
2a SECURITY CLASSIFICATION AUTHORITY N/A		3 DISTRIBUTION/AVAILABILITY OF REPORT Approved for public release; distribution unlimited												
2b DECLASSIFICATION/DOWNGRADING SCHEDULE N/A														
4. PERFORMING ORGANIZATION REPORT NUMBER(S) N/A		5 MONITORING ORGANIZATION REPORT NUMBER(S) RADC-TR-86-133												
6a. NAME OF PERFORMING ORGANIZATION Rensselaer Polytechnic Institute	6b OFFICE SYMBOL (if applicable)	7a NAME OF MONITORING ORGANIZATION Rome Air Development Center (RBRP)												
6c. ADDRESS (City, State, and ZIP Code) 110 8th Street Troy NY 12181		7b ADDRESS (City, State, and ZIP Code) Griffiss AFB NY 13441-5700												
8a. NAME OF FUNDING/SPONSORING ORGANIZATION AFOSR	8b OFFICE SYMBOL (if applicable) NE	9 PROCUREMENT INSTRUMENT IDENTIFICATION NUMBER F30602-83-C-0194												
8c. ADDRESS (City, State, and ZIP Code) Bolling AFB Wash DC 20332		10 SOURCE OF FUNDING NUMBERS <table border="1"><tr><td>PROGRAM ELEMENT NO 61102F</td><td>PROJECT NO 2306</td><td>TASK NO J4</td><td>WORK UNIT ACCESSION NO 16</td></tr></table>				PROGRAM ELEMENT NO 61102F	PROJECT NO 2306	TASK NO J4	WORK UNIT ACCESSION NO 16					
PROGRAM ELEMENT NO 61102F	PROJECT NO 2306	TASK NO J4	WORK UNIT ACCESSION NO 16											
11 TITLE (Include Security Classification) COMPUTER SIMULATION OF DETERIORATION BY ELECTROMIGRATION														
12 PERSONAL AUTHOR(S) H. B. Huntington, S. Ahmad														
13a. TYPE OF REPORT Final	13b. TIME COVERED FROM Nov 83 TO May 85	14. DATE OF REPORT (Year, Month, Day) September 1986	15 PAGE COUNT 20											
16. SUPPLEMENTARY NOTATION N/A														
17. COSATI CODES <table border="1"><tr><th>FIELD</th><th>GROUP</th><th>SUB-GROUP</th></tr><tr><td>14</td><td>04</td><td></td></tr><tr><td></td><td></td><td></td></tr></table>		FIELD	GROUP	SUB-GROUP	14	04					18 SUBJECT TERMS (Continue on reverse if necessary and identify by block number) Electromigration Simulation <i>X</i>			
FIELD	GROUP	SUB-GROUP												
14	04													
19 ABSTRACT (Continue on reverse if necessary and identify by block number) Analysis of electromigration and redistribution of material in grain boundaries has been programmed for simulation of these processes in relatively realistic grain boundary networks generated from computer generated Voronoi networks. Realism is improved by simulation of annealing prior to simulation of electromigration.														
20. DISTRIBUTION/AVAILABILITY OF ABSTRACT <input checked="" type="checkbox"/> UNCLASSIFIED/UNLIMITED <input type="checkbox"/> SAME AS RPT <input type="checkbox"/> DTIC USERS			21 ABSTRACT SECURITY CLASSIFICATION UNCLASSIFIED											
22a. NAME OF RESPONSIBLE INDIVIDUAL Mark W. Levi			22b. TELEPHONE (Include Area Code) (315) 330-2075	22c. OFFICE SYMBOL RADC (RBRP)										

Evaluation

This work has provided some much needed analysis of the conditions of electromigration in models of greater realism than have heretofore been attacked. The progress has been good considering the complexity and ambitiousness of the task. Further effort would be well advised.

Mark W. Levi (m)

MARK W. LEVI
Project Engineer



<input checked="" type="checkbox"/>	<input type="checkbox"/>	<input type="checkbox"/>
<input type="checkbox"/>	<input type="checkbox"/>	<input type="checkbox"/>
<input type="checkbox"/>	<input type="checkbox"/>	<input type="checkbox"/>
<input type="checkbox"/>	<input type="checkbox"/>	<input type="checkbox"/>
Classification Codes		
Approved by/		
Date _____		
<i>A-1</i>		

I. Planning and Survey Stage

The work began with a computer search for relevant material published during the last two years in the Chemical Abstracts and Physics Abstracts. From the Chemical Abstracts a total of 113 references responded to a call from the key words "electromigration" and "electrotransport". These were surveyed for applicability and availability and 26 rated high on both counts. The corresponding reference list was much longer for the Physics Abstracts. It was decided to require also mention of "thin film" as a key phrase and this reduced the list substantially - to 25. All seemed pertinent and were provided with substantial abstracts. There was naturally a considerable degree of overlap between the two lists. This background has proved most useful in selecting a topic for in depth study and also in giving a general picture of the most recent aspect of electromigration problems.

II. Generation of Grain Boundary Network.

In the course of this literature survey there surfaced one particularly pertinent paper by K. Nikawa¹, which described a detailed computer simulation, using Monte Carlo methods, of a rather simplified model of stripe deterioration by grain boundary transport. The accompanying reference list 2-5 includes several earlier papers in the general field. It was in this area we decided to concentrate our computing efforts.

The first step in this procedure was to devise a system for generating a realistic grain boundary network. This was planned as a two step process.

A. First a random network of grains was generated according to the Voronoi prescription, which has been discussed in a review article by Weaire and Rivier⁶. The method is to establish a random placing of points in two dimensions. Next one constructs the perpendicular bisectors between all pairs of adjacent points and portions of these lines now constitute the grain boundaries of the network. The physical interpretation could be that the random points correspond to nucleation centers for crystallization which grow uniformly until they meet at the

perpendicular bisectors, i.e. grain boundaries. In programming this concept for a stripe of a particular width we made use of a prior program⁷ by I. K. Crain for a limited network and were successful in generating reasonable structures for different size grains. As a last step grain orientations were established by Monte Carlo selection.

B. Next an effort was made to equilibrate the intergranular tensions at the vertices of the network. We assumed that these tensions would practically equal to the intergranular energies (on the assumption of negligible temperature dependence). For these energies a dislocation model was again invoked which set the grain boundary energy proportional to the dislocation density or $\sin^2 \theta$ for $\theta < 37^\circ$ and kept the energy constant for $\theta > 37^\circ$, where θ is the angle of misorientation between the adjacent grains. Since the grain boundary diffusivity also varies in somewhat the same way as the tension, it seemed desirable, perhaps even important, to try to establish tension equilibration. This proved, however, quite a difficult business, as might have been anticipated for a multidimensional search for a equilibrium configuration. For a time this effort was shelved in favor of an exploration of the actual mass motions with the grains.

III. Modelling the Electromigration Process

A. Characteristics of the grain boundaries

The key quantity in the simulation process is $m_\sigma(x, t)$, the amount of matter in grain boundary segment (denoted by subscript σ) per unit length. Initially all grain boundaries are assumed ungrooved and the m_σ have a constant value $m_0 = N d_0 \delta$ where N is the number of atoms per unit volume, d_0 is the thickness of the stripe film and δ is the (nominal) width of the grain boundary segment. In some regions $m_\sigma > m_0$ and there is matter build-up which continues until $m_0 \sim m_M$ at which point extrusion starts. In contrast to those grain boundaries which show matter excess there are others which show matter deficit $m_\sigma < m_0$. Because these regions are critical in void formation their treatment is more detailed and complex. Matter deficit in the grain boundaries (vacancies) tends to condense

as grain boundary grooves at the surface. As we show later, the number of vacancies still in the grain boundary is relatively small after a short initial period. The matter missing in the grain boundary grooves, per unit length of grain boundary, is taken to be $Nd_g^2 \tan \beta$ ($\tan \beta$ is small and has been arbitrarily set at 0.1) where d_g is the depth of the groove and β is the angle at the groove base.

With the appearance of the grooves another mechanism for mass transport becomes operative - surface motion down the groove walls. (Presumably surface diffusion over the upper surface of the stripe is inhibited by a passivating layer.) This process should proceed rapidly and be independent of the original grain misorientation at the boundary. Its effect is to widen the groove and therefore a new quantity, $w(x, t)$, is introduced which denotes the grain boundary width at the surface for each point along the segment. This action greatly increases the effective β so that $\beta + \beta'$ where $\tan \beta' = -\frac{w}{2d_g}$

In addition to the $m(x, t)$ quantities to describe the state of the segment, one might also consider $g(x, t)$, the groove volume per unit length. It appears, however, that, in general, $g(x, t) \neq (m_0 - m(x, t))$ will be close to unity, since the vacancy volume in the grain boundary is relatively small.

B. Equations for mass motion

Within the grain boundary the appropriate mass transport equation is

$$\frac{\partial m(x, t)}{\partial t} = \frac{\partial}{\partial x} \{ D_{\sigma 1} \left[\frac{\partial m(x, t)}{\partial x} - A m(x, t) \right] \} \quad (1)$$

Distance along the grain boundary segment is denoted by x . The grain boundary diffusivity is $D_{\sigma 1}$ where σ again numbers the segment. We show in next section $D_{1\sigma}(\theta)$, where θ is the misorientation angle between the grains meeting to form the boundary. The coefficient of the driving force term, A , is $A_0 \cos \phi$ where ϕ is the angle between the grain boundary and direction of E and A_0 is $\frac{|e|EZ^*}{kT}$ about $0.1 \mu\text{m}$ for $E = 2.2 \text{V/cm}$, $Z^* = 20$ and $T \sim 150^\circ \text{C}$. All changes in m are treated on an equal basis, whether they arise from changes of vacancy concentration in the

grain boundary or a gradient in groove depth.

Preparatory to setting the equation up for computer application each segment had its length divided into a discrete number of evenly spaced check points. The spacing is denoted by a and is roughly about $0.2\mu\text{m}$ for all segments.

Eq (1) is now written

$$\frac{\partial m(x,t)}{\partial t} = \frac{D_{1\sigma}}{a} \left[\frac{m_{n+1} - 2m_n + m_{n-1}}{a} - \frac{m_{n+1} - m_{n-1}}{2} A_\sigma \right] \quad (1a)$$

Where the digitized values for m have been used on the right. At the ends of the segments ($n = 0$ or n_t) the equation is slightly altered.

$$\frac{\partial m(0,t)}{\partial t} = \sum_\sigma \frac{D_{1\sigma}}{a} \left[\frac{m_1 - m_0}{a} - A_\sigma m_1 \right] \quad (1b)$$

In a similar way the surface motion on the groove walls can be expressed in terms of $g(x, t) = N \times$ volume of the groove/length.

$$\frac{\partial g(x,t)}{\partial t} = \frac{\partial}{\partial x} D_s \left[\frac{\partial g(x,t)}{\partial x} - A_s g(x,t) \right] \quad (2)$$

Where D_s is the diffusion on the free surface and A_s is the surface driving force. As before the digitized version is

$$\frac{\partial g}{\partial t} = \frac{D_s}{a} \left[\frac{g_{n+1} - 2g_n + g_{n-1}}{a} - A_s \frac{g_{n+1} - g_{n-1}}{2} \right] \quad (2a)$$

and for the segment ends

$$\frac{\partial g_0}{\partial t} = \frac{D_s}{a} \left[\frac{g_1 - g_0}{a} - A_s g_1 \right] \quad (2b)$$

(In a later section we give an argument why the diffusion term should be omitted from eq. 2.)

C. Assumed stripe structure

It is reported that most metallized stripes, particularly for aluminum, exhibit a pronounced $\{111\}$ structure. Such a structure implies that

pure tilt interfaces constitute most of the grain boundaries. If we invoke a dislocation model for the small angle grain boundaries, these would then consist of edge dislocations directed perpendicular to the substrate, hence the notation D_{10} for diffusion in the stripe, perpendicular to the dislocations. Accordingly the assumption is made that for large angle grain boundaries ($\theta > 37^\circ$ as a nominal dividing line), diffusion is isotropic at a value D_1 . Holding to the dislocation model for grain boundaries one obtains for the diffusion parallel to the dislocation and directed perpendicular to the substrate

$$D_{\parallel} = D_1 \sin \theta/2 / \sin 37^\circ/2 \quad \text{for } \theta < 37^\circ \quad (3)$$

For diffusion along the stripe one modifies a formula of Li to get

$$\frac{1}{D_{\perp}} = \frac{1-\alpha_0}{D_0} + 6 \frac{\alpha_0}{D_1} \quad (4)$$

where D_0 is the diffusion through the bulk and $\alpha_0 = r_0/h$. Here r_0 is the dislocation core radius, $b/h = 2 \sin \frac{\theta}{2}$ and b is the Burgers vector. (The original

Li formula was $\frac{1}{D} = \frac{1-\alpha_0}{D_0} + \frac{\alpha_0}{(1-\alpha_0)D_0 + \alpha_0 D_1}$). Nominally $\alpha_0 = \frac{\sin \theta/2}{\sin 37^\circ/2}$.

D. Difficulty with Diffusion

The direct integration of equs (1) and (2) poses a problem in that useful convergence of the diffusion part requires some subtlety in method and a very considerable number of time steps. In terms of an average segment length L_{Av} the natural time constants of the system are $[D_1 L_{Av}^{-2}]$ (about $.6 \times 10^3$ s) and $[D_1 A L_{Av}^{-1}]$ (about 5×10^3 s). As both of these constants are very short, of the order of an hour, it is clear that the approach to void formation must not be limited to time steps of such small size. Accordingly a procedure was developed to integrate over a longer period.

E. Steps in the program simulation

The individual stages that are involved in each time step are here described in order, somewhat after procedure used in the twelfth status report.

a.) First stage - matter accumulation (or depletion) at each vertex, F_v , in accord with eq (1b),

$$F_v = \sum_{\sigma} D_{\sigma\perp} \left[\frac{(m_1 - m_0)}{a} - A_{\sigma} m_1 \right],$$

where the σ -summation is over the segments which meet at the vertex in question. For the first time-step all the m 's are equal and only the A_{σ} term contributes.

b.) Redistributing F_v among the segments meeting at V .

For each segment a portion of F , namely f_{σ} , is redistributed as a flux coming into the segment.

$$f_{\sigma} = F_v D_{\sigma\perp} \frac{1}{2} / \sum_{\sigma} D_{\perp\sigma} \frac{1}{2} \quad (5)$$

c.) Method of redistribution

The thin film solution for the diffusion equation is used, working from both ends of the segment,

$$a \frac{\partial m(x, t)}{\partial t} = f_{\sigma} \frac{1}{(\pi D_{\perp\sigma} t)^{\frac{1}{2}}} e^{-x^2/4D_{\perp\sigma} t} \quad (6)$$

One would like to be able to state what $m(x, t)$ is at time t .

Integration gives $m(x, t_1) = (\pi)^{\frac{1}{2}} f_{\sigma} D_{\sigma}^{-1} x \zeta \left(\frac{x}{2(D_{\sigma} t_1)^{\frac{1}{2}}} \right)$ where $\zeta(y) = \frac{e^{-y^2}}{y} - \sqrt{\frac{\pi}{2}} \operatorname{erfc} y$.

This integration technique allows one to greatly increase the time, from 10^4 to 10^6 seconds. For such long times, however, the diffusion thin-film solution will usually have a large value at the opposite end of the segment. These "tails" have to be evaluated by integrating $m(x)$ from x_1 to ∞ ,

$$\int_{x_1}^{\infty} m(x) dx = \frac{2f}{\pi} \frac{1}{2} t_1 n(y_1) = T(x_1, t_1) \quad (7)$$

$\frac{x_1}{}$

where $n(y_1) = (1 + 2y_1^2) \int_{y_1}^{\infty} e^{-y^2} dy - y_1 e^{-y_1^2}$ and $y_1 = 2 \sqrt{\frac{D_{\sigma}}{\sigma} t_1}$. One then sums the $T(L_{\sigma}, t)$ at each vertex for the "tail" contribution from all the segments that meet there. This gives a new F_2 which is then iterated to give smaller contributions to the $m_{\sigma}(x, t_1)$ of the network.

d.) After these "tailing" corrections have converged, the next stage is to consider the grooving that occurs near those vertices where a material deficit has developed. If $m(x, t_1) - m_0 < 0$, it is reasonable to expect large fraction of this deficit will be converted into the grain boundary groove volume, $g(x, t_1)$, or

$$g(x, t_1) = K(x, t_1) \{m_0 - m(x, t_1)\} = K(x, t_1) m_1(x, t_1) \quad (8)$$

$K(x, t_1)$ can be estimated from a model wherein the diffusion of vacancies in the z -direction (upward from the substrate) is explored. Suppose $m(x, z, t_1) = m(x, t_1) Z(z)$ where

$$Z(z) = -\frac{\pi}{2d_b} \cos \frac{\pi z}{2d_b} \quad (9)$$

Here $z = 0$ at the substrate and $z = d_b$ at the bottom of the groove, $d_b = d_0 - d_g$ where d_g is the groove depth. Introduce now $T(x, t_1)$, the number of vacancies still in the grain boundary, $T(x, t_1) = m_1(x, t_1) - g(x, t_1)$

$$\frac{\partial T(x, t)}{\partial t} = -\lambda \frac{m(x, t)}{\sigma} + \frac{1}{\partial t} \quad (10)$$

Here $\lambda = D_{\sigma}(\theta) \left(\frac{\pi}{2d_b} \right)$ from the equation for diffusion perpendicular to the

substrate and $\frac{\partial m_1}{\partial t}$ could be taken from (eq 6) - if tailing correction is neglected.

To get a rough solution disregard the Gaussian factor since long times are

involved. Roughly then $\frac{\partial m_1}{\partial t} \sim A t^{-\frac{1}{2}}$ and $m \sim 2A(t_1^{\frac{1}{2}} - t_m^{\frac{1}{2}})$ when t_m is a short time cut-off which replaces the exponential.

$$\frac{\partial T}{\partial t} = -\lambda T + A e^{\frac{1}{2}} \quad (10a)$$

Discarding the homogeneous solution $ce^{-\lambda t}$ we have for T

$$T(t) = Ae^{-\lambda t} \int_{t_m}^{t_1} e^{t' \lambda} (t_1 - t')^{-\frac{1}{2}} dt' = A \int_0^{t_1} e^{-\lambda \tau} \tau^{-\frac{1}{2}} d\tau$$

$$T(t) = 2A \times -\frac{1}{2} [\operatorname{erf}(\lambda^{\frac{1}{2}} t_1) - \operatorname{erf}(\lambda^{\frac{1}{2}} t_m)] \sim 2A \lambda^{-\frac{1}{2}}$$

and finally $K(x,t) \approx \{1 - (\lambda t_1)^{-1}\} \quad (11)$

Often $K(t)$ is close enough to unity to neglect the difference. Actually the form

of (9) is quite independent of the formula for $\frac{\partial m_1}{\partial t}$. To determine d_g the groove

depth we assume it to be V-shaped with a small vertex angle β . Then

$$g(x) = N d_b^2 \tan \beta \quad (12)$$

e.) The treatment of the surface diffusion along the walls of grooves bears a close resemblance to the procedure of the earlier sections dealing with diffusion in the grain boundaries. We use the results of section D for d_g to determine F_{sv} , the quantity analogous to F_v of section (a)

$$F_{sv} = - \sum_s D_s A_{s\sigma} \frac{2d_{gov}}{g_{gov}} \sec \beta. \quad (13)$$

Here D_s is the surface diffusivity which characterizes the free surface. (Our model presumes that, without grooving, there is no free surface because of oxydizing or passivating films.) The $A_{s\sigma}$ is the driving force coefficient for the surface and equals $A_s \cos \phi_\sigma$. The $d_{g\sigma}$ is the groove depth for the σ segment at the V vertex. The diffusion contributions to (11) have been omitted since the surfaces of the groove walls are smooth and there is no preferred direction for matter diffusion. It is implied that there is no electromigration-driven pile-up of vacancies along the groove wall surfaces.

As before the F_{sv} is divided into $f_{s\sigma}$, which are now all equal since D_s is independent of σ . The back distribution into the segments now gives rise to two different possibilites: segments that show deficits at both ends and those which show deficit at one end only. Without the pure diffusion term the mass motion equation becomes

$$\frac{\partial G_\sigma(x,t)}{\partial t} = -D_s A_{s\sigma} \frac{\partial G_\sigma(x,t)}{\partial x} \quad (2c)$$

The quantity $G(x,t)$ is that groove volume, over and above $g(x,t)$ previously defined, which is acquired by virtue of the surface mass motion.

A useful long time solution for this equation is

$$G_g(x,t) = B_1 - B_2 x + B_2 D_s A_{st} \quad (14)$$

where B_1 and B_2 coefficients are fitted to flux conditions at the vertices or zero flux condition for those grooves that terminate in a segment (single-ended grooves). If we hold to the V-shaped groove model then $G = d_g \tan \beta'$ where now $\beta' \gg \beta$ and β' may be a large angle. The details of the solution of this surface aspect have not yet been completely worked out.

f.) The regions of material excess require less detail than those showing deficit. We expect to select a criterion for the breaking of the passivating layer by internal pressure. After this is exceeded the local mass build-ups with time will cease as the extra material is extruded.

F. Present situation and future directions.

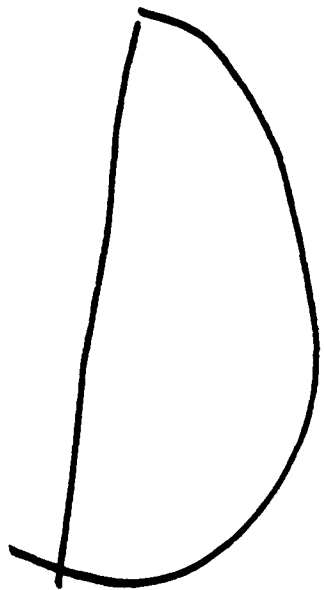
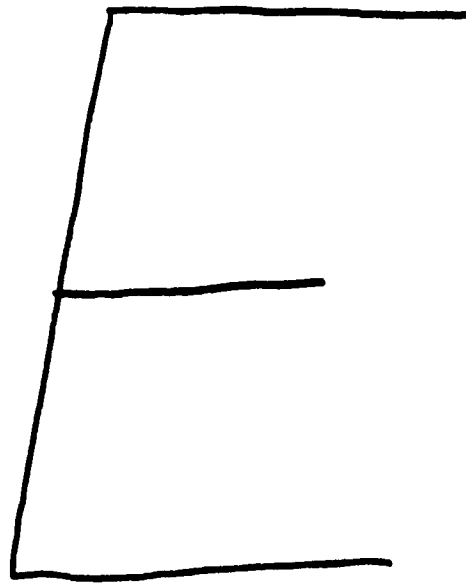
Programming has proceeded to the point of stage c, as detailed in section E. Trial runs on a single grain have proved satisfactory. Further work should incorporate the remaining stages and enlarge the operating field to a full stripe. As one proceeds with ensuing time steps the grooves become incised deeper and surface diffusion replaces grain boundary diffusion as the principal mode of mass transport. For the cases where voids have developed a somewhat different program of operations will be needed. It is quite problematical how to bring consideration of electrical and thermal effects into play but they certainly should be considered.

References

1. "Monte Carlo Calculations Based on the Generalized Electromigration Failure Model", by Kiyoshi Nikata. Reliability Physics Symposium Annual Proceedings, 19, 175-81 (1981).
2. "Statistical metallurgical model for electromigration failure in aluminum thin film conductors" by N. J. Attardo, R. Rutledge and R. C. Jack, J. Appl. Phys. 42, 4343 (1971).
3. "A statistical model for electromigration induced failure", by J. D. Venables and R.G. Lye, IEEE, Proc. 10 IRPS, 159 (1972).
4. "Electromigration and metallization lifetimes", by R. A. Sigsbee, J. Appl. Phys. 44 2533 (1973).
5. "Monte Carlo calculations of structure-induced electromigration failure" by J. M. Schoen, J. Appl. Phys. 51, 513 (1980).
6. "Soaps, cells, and Statistics - Random Patterns in Two Dimensions" by D. Weaire and N. Rivier, Contemp. Phys., 25, 59-99 (1984).
7. "The Monte-Carlo Generation of Random Polygons" by I. K. Crain, Computers and Geophysics, 4, 131-141 (1978).
8. "High Angle Tilt Boundary - A Dislocation Core Model" by James C. M. Li, J. Appl. Phys. 32, 525 (1961).

MISSION
of
Rome Air Development Center

RADC plans and executes research, development, test and selected acquisition programs in support of Command, Control, Communications and Intelligence (C³I) activities. Technical and engineering support within areas of competence is provided to ESD Program Offices (POs) and other ESD elements to perform effective acquisition of C³I systems. The areas of technical competence include communications, command and control, battle management, information processing, surveillance sensors, intelligence data collection and handling, solid state sciences, electromagnetics, and propagation, and electronic, maintainability, and compatibility.



3 —

8 1

Dtic